DRUG DEVELOPMENT

Structure-switching aptamer sensors for the specific detection of piperaquine and mefloquine

Erin S. Coonahan[1,2,3]*, Kyung-Ae Yang[4], Stevan Pecic[5], Maarten De Vos[2,6,7], Thomas E. Wellems[1], Michael P. Fay[8], John F. Andersen[1], Joel Tarning[3,9], Carole A. Long[1]†

Copyright © 2021 The Authors, some rights reserved; exclusive licensee American Association for the Advancement of Science. No claim to original U.S. Government Works

Tracking antimalarial drug use and efficacy is essential for monitoring the current spread of antimalarial drug resistance. However, available methods for determining tablet quality and patient drug use are often inaccessible, requiring well-equipped laboratories capable of performing liquid chromatography–mass spectrometry (LC-MS). Here, we report the development of aptamer-based fluorescent sensors for the rapid, specific detection of the antimalarial compounds piperaquine and mefloquine—two slow-clearing partner drugs in current first-line artemisinin-based combination therapies (ACTs). Highly selective DNA aptamers were identified that bind piperaquine and mefloquine with dissociation constants (K_d's) measured in the low nanomolar range via two independent methods. The aptamers were isolated from a library of single-stranded DNA molecules using a capture–systematic evolution of ligands by exponential enrichment (SELEX) technique and then adapted into structure-switching aptamer fluorescent sensors. Sensor performance was optimized for the detection of drug from human serum and crushed tablets, resulting in two sensing platforms. The patient sample platform was validated against an LC-MS standard drug detection method in samples from healthy volunteers and patients with malaria. This assay provides a rapid and inexpensive method for tracking antimalarial drug use and quality for the containment and study of parasite resistance, a major priority for malaria elimination campaigns. This sensor platform allows for flexibility of sample matrix and can be easily adapted to detect other small-molecule drugs.

INTRODUCTION

Despite substantial efforts over the last several decades, more than 1 billion people worldwide still live at risk of malaria infection (*1*). In 2019, there were more than 200 million global cases of malaria and more than 400,000 associated deaths, most of which occurred in children under 5 years of age (*2*). *Plasmodium falciparum* is the most prevalent and deadliest malaria species worldwide. The current first-line treatment for *P. falciparum* malaria is a combination of a fast-acting artemisinin derivative and a slower-clearing partner compound. These artemisinin-based combination therapies (ACTs) combine the rapid parasite clearance of artemisinin with the lasting effects of longer half-life partner compounds to prevent recrudescences and counter emerging parasite resistance.

However, over the last decade, parasite resistance to several slow-clearing ACT partner drugs has emerged in Southeast Asia leading to the inability of the ACT to successfully cure malaria infections (*3*). Reduced parasite susceptibility to dihydroartemisinin (DHA)–piperaquine was first reported in 2008 along the Thai-Cambodia border (*4*, *5*). In 2015, as a result of high DHA-piperaquine failure rates, Cambodia's first-line therapy was switched to artesunate-mefloquine, an alternate ACT (*6*, *7*). From 2008 to present, DHA-piperaquine–resistant parasites have spread from the Thai-Cambodia border across most of Southeast Asia (*8*). This pattern of spread is not unique to current first-line therapies. In the late 20th century, parasites resistant to chloroquine, sulfadoxine, and pyrimethamine spread westward from Southeast Asia to eventually reach the African continent (*3*, *9*, *10*). As a result of spreading chloroquine resistance during a time of population growth, global malaria deaths almost doubled from roughly 1 million reported deaths in 1980 to more than 1.8 million in 2004 (*11*). This trend highlights the need for close monitoring of ACT efficacy and the spread of resistance to partner drugs, especially in Africa where the majority of the malaria burden exists and where ACTs, including DHA-piperaquine, currently remain effective.

Measuring ACT content in patient blood samples and tablets is essential for studying drug use practices and identifying counterfeit therapies—both believed to be important contributors to the emergence and spread of resistance. The standard method for measuring antimalarial drug quantities for pharmacokinetic analysis, surveillance, and tablet quality assessment is liquid chromatography–mass spectrometry (LC-MS). Over the past 20 years, methods to extract and measure commonly used antimalarial drugs from dissolved tablets and patient samples have been optimized in several laboratories around the world (*12*–*17*). These methods can be extremely sensitive and accurate but require shipping samples to such a laboratory capable of performing the analysis, which is both time-consuming and costly. Sample stability during shipment is inconsistent and cold chain shipments can be prohibitively expensive and logistically challenging. To avoid the shipment of frozen blood or plasma, several methods to extract antimalarial drugs from dried blood spots have been developed (*18*, *19*). However, these methods still require substantial financial resources and access to the very few laboratories worldwide with the expertise to run LC-MS protocols for the detection of antimalarial drugs.

[1]Laboratory of Malaria and Vector Research, NIAID, NIH, MD 20892-8132, USA. [2]Institute of Biomedical Engineering, University of Oxford, Oxford OX3 7DQ, UK. [3]Mahidol Oxford Tropical Medicine Research Unit, Faculty of Tropical Medicine, Mahidol University, Bangkok 10400, Thailand. [4]Department of Medicine, Columbia University, New York, NY 10032, USA. [5]Department of Chemistry and Biochemistry, California State University , Fullerton, CA 92831, USA. [6]Department of Electrical Engineering (ESAT), KU Leuven, Leuven 3000, Belgium. [7]Department of Development and Regeneration, KU Leuven, Leuven 3000, Belgium. [8]Biostatistics Research Branch, DCR, NIAID, NIH, Rockville, MD 20852, USA. [9]Centre for Tropical Medicine and Global Health, Nuffield Department of Medicine, University of Oxford, Oxford OX3 7LG, UK.
*Present address: University of California San Diego, School of Medicine, San Diego, CA 92093, USA.
†Corresponding author. Email: clong@niaid.nih.gov

Downloaded from http://stm.sciencemag.org/ by 60259981 on March 17, 2021

Systematic evolution of ligands by exponential enrichment (SELEX) is a procedure to find aptamer sequences that bind specific target molecules. SELEX protocols require a library of synthetic DNA or RNA sequences with conserved primer regions flanking 20 to 80 random bases. The random region provides variability in folding and charge distribution to allow interaction with various targets, while the primer regions facilitate amplification of the library via polymerase chain reaction (PCR). The library is repeatedly exposed to desired targets, and target binding sequences are sorted and amplified through each round until the pool evolves to contain sequences with desired characteristics. Like protein antibodies, aptamers demonstrate target binding sensitivity and specificity required for many biosensing and therapeutic applications. However, aptamers have several advantages over antibodies including room temperature stability, in vitro isolation, and superior differentiation between small-molecule targets (*20*, *21*).

Small molecule–binding aptamers are appealing owing to their potential for impressive specificity. However, aptamer selection against small-molecule targets carries additional challenges compared to protein targets. Small molecules have less surface area, less structural diversity, and fewer available binding motifs than typical protein targets, and they can be difficult to immobilize for sequence sorting during SELEX, requiring chemical modifications that may inhibit the identification of high-affinity aptamers against native targets (*20*). From the invention of aptamers in 1990 through 2015, proteins accounted for more than 70% of all published aptamer targets, whereas small-molecule targets made up less than 20% (*22*–*24*).

A SELEX technique called capture-SELEX circumvents several small-molecule selection challenges by immobilizing the aptamer library rather than the target molecule to a solid support via a short complementary oligo (*25*). Aptamer sequences that fold to release the short complementary oligo and bind free target are collected and advanced to further rounds. The selection of aptamers that undergo a conformational change upon target binding is especially desirable for later adaptation into sensing platforms (*26*). Using variations of the capture-SELEX protocol, aptamer sensors have been developed for the detection of diverse small-molecule targets including monosaccharides, amino acids, and drug compounds (*27*–*29*).

An inexpensive assay to detect antimalarial compounds from patient samples and dissolved tablets implemented in malaria clinics or small research laboratories could greatly improve the collection of drug use and quality data. After ACT administration, the long half-life partner drug components are detectable in patient blood samples up to several weeks after treatment, in contrast to artemisinin derivatives and their metabolites, which clear from the blood within a day (*30*–*35*). Piperaquine and mefloquine were selected for detection in this research due to their widespread use and failures against resistant *P. falciparum* strains in Southeast Asia. To detect and differentiate between these and similarly structured small-molecule drugs, we identified selectively binding DNA aptamers from oligonucleotide libraries and adapted them into structure-switching fluorescent sensors.

RESULTS

Selection of specific piperaquine and mefloquine aptamers for sensor via SELEX

DNA aptamers with selective binding affinity for either piperaquine or mefloquine were identified using a capture-SELEX method (*26*). Conditions were optimized to reduce cross-reactivity to similarly structured quinoline antimalarials and human serum components. Several iterations of SELEX experiments were performed, each consisting of 15 to 20 rounds. The SELEX protocol used a short biotinylated capture oligonucleotide to adhere aptamer libraries to a streptavidin agarose solid support. The immobilized libraries were then exposed to rounds of negative and positive selection in which preparations of potentially interfering substances including human serum and similarly structured antimalarial drugs (negative selection) or solutions of the desired antimalarial target (positive selection) were loaded onto the column (Fig. 1A). SELEX conditions and round-specific target concentrations are provided in tables S1 and S2.

After each round of SELEX, the collected positive selection pools were amplified via PCR, denatured with alkaline solution to regenerate a single-stranded library, and then loaded onto a new column via hybridization to the biotinylated capture oligo for a subsequent round. SELEX progress was monitored via tracking DNA elution profiles, which informed selection conditions and SELEX completion (Fig. 1B). After the final SELEX round, aptamer pools were cloned and sequenced, and results were sorted based on sequence enrichment and degree of similarity (Fig. 1C) (*36*). The most promising aptamers were identified as having both sufficient target affinity and specificity. During SELEX, only aptamer sequences that fold to interact with drug targets, releasing from the solid support, were collected. This requirement that binding DNA sequences must undergo a structural change resulting in a release from a complementary capture oligo ensured that resulting aptamer sequences could be easily adapted into a simple fluorescent sensor by conjugating a fluorophore to the aptamer and replacing the capture strand's biotin tag with a small-molecule quencher (Fig. 1D). Using this sensor design, preparation of the final assay for drug detection from serum or plasma requires three steps, with sample preparation consisting of only a dilution step. The steps to perform a drug content measurement are schematically presented in Fig. 1E.

The most promising piperaquine and mefloquine binding aptamers were characterized by surface plasmon resonance using a Biacore T100. The aptamer two-dimensional (2D) folding structures with the lowest free energy, as predicted by Mfold (*37*), are shown in Fig. 2A. Additional, higher-energy, potential folding structures are reported in fig. S1. Single-cycle Biacore sensorgrams are shown in Fig. 2B. The most promising piperaquine aptamer (PQ4) reported a K_d of 2.43 nM and the most promising mefloquine aptamer (MQ2) reported a K_d of 19.2 nM (Fig. 2C) via Biacore. Supplementary Biacore experiments reporting very similar K_d values within expected run-to-run variability corroborate these results and are included in fig. S2.

In addition, an alternative method to calculate K_d values using fluorescent sensor saturation curves is presented in Fig. 2D. In this method, a dissociation constant for the capture oligonucleotide with the drug-binding aptamers is first determined. Then, the target-induced aptamer-quencher dissociation is measured, and a dissociation constant for aptamer-target binding is calculated from the two equilibrium constants (*26*, *38*). The results provide a second independent physical method to report K_d values that differ by only two- to threefold those reported via Biacore. On the basis of these results, we are confident that the K_d values reported are all within the low nanomolar range, providing necessary sensor sensitivity for clinical applications.

Downloaded from http://stm.sciencemag.org/ by 60259981 on March 17, 2021

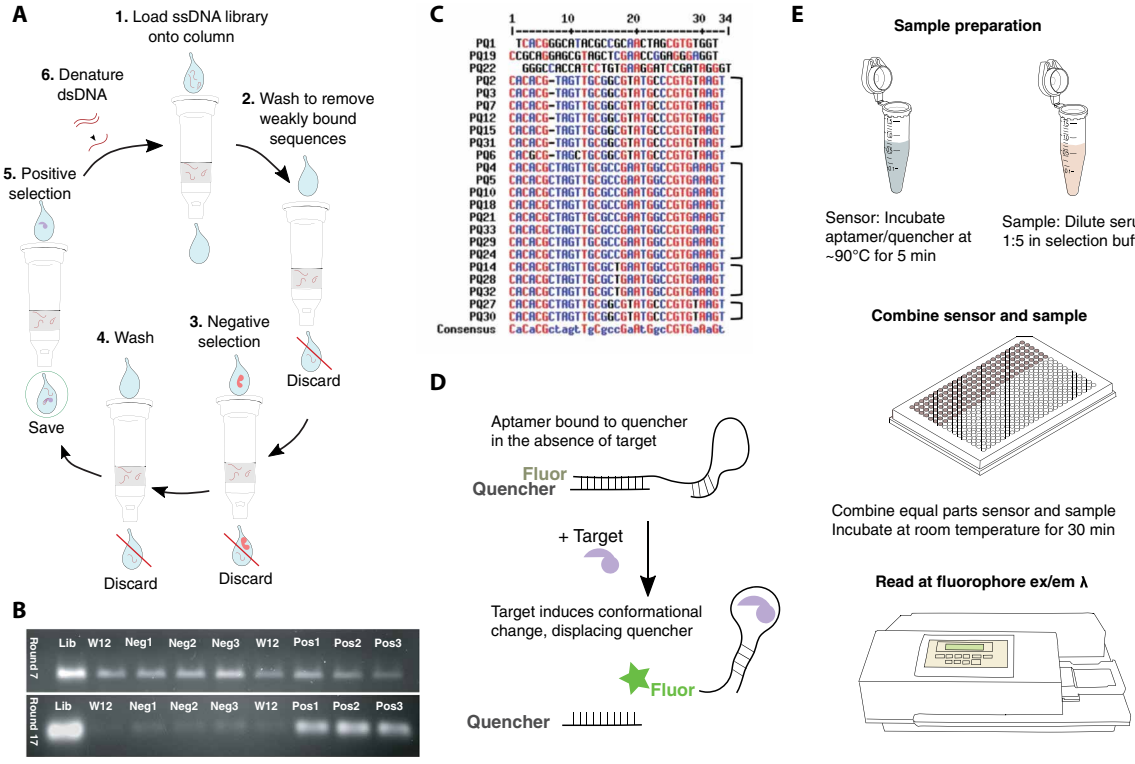


Fig. 1. Aptamer selection, sensor design, and assay workflow. (**A**) Column-based capture-SELEX protocol (*26*). Each iteration constitutes one round of SELEX. (**B**) Monitoring SELEX progress via elution profiles. DNA eluted from the column during final washes (W12), negative (Neg 1, 2, and 12), and positive (Pos 1 to 3) selection steps as well as a sample of initial library loaded on the column (Lib) from each round were amplified via PCR and then run together on an agarose gel for visual comparison of the amount of DNA eluted in each step. The top gel shows an elution profile from round 7 of piperaquine SELEX, whereas the bottom gel is from round 17. (**C**) Sequencing results of a final library pool from piperaquine aptamer selection. Sequences of interest were selected based on copy number and predicted folding. Brackets indicate identical sequences. Red indicates >90% and blue indicates >50% base identity across sequences, displayed using Multalin Sequence Alignment Software. (**D**) Design of the aptamer sensor. Final sequences identified after capture-SELEX were adapted into fluorescent sensors by attaching a quencher molecule to the complementary oligo and a fluorophore to the aptamer. In the absence of target, the fluorophore is quenched and the magnitude of fluorescence response correlates with target concentration. (**E**) Aptamer assay workflow. To prepare the sensor, an aptamer/quencher stock is resuspended in selection buffer according to the desired aptamer:quencher ratio, incubated at ~90°C for 5 min to promote proper folding, and allowed to cool to room temperature. To prepare the sample, plasma, serum, or dissolved tablets are diluted in selection buffer. Sensor and sample are combined in a 1:1 ratio in a fluorescent well plate, allowed to equilibrate for ~30 min, and then read on a standard fluorimeter. A standard curve of drug target should be run on each plate for interpolation of concentration values. Ex/em λ: excitation/emission wavelengths.

Development and characterization of fluorescent aptamer sensor in human samples

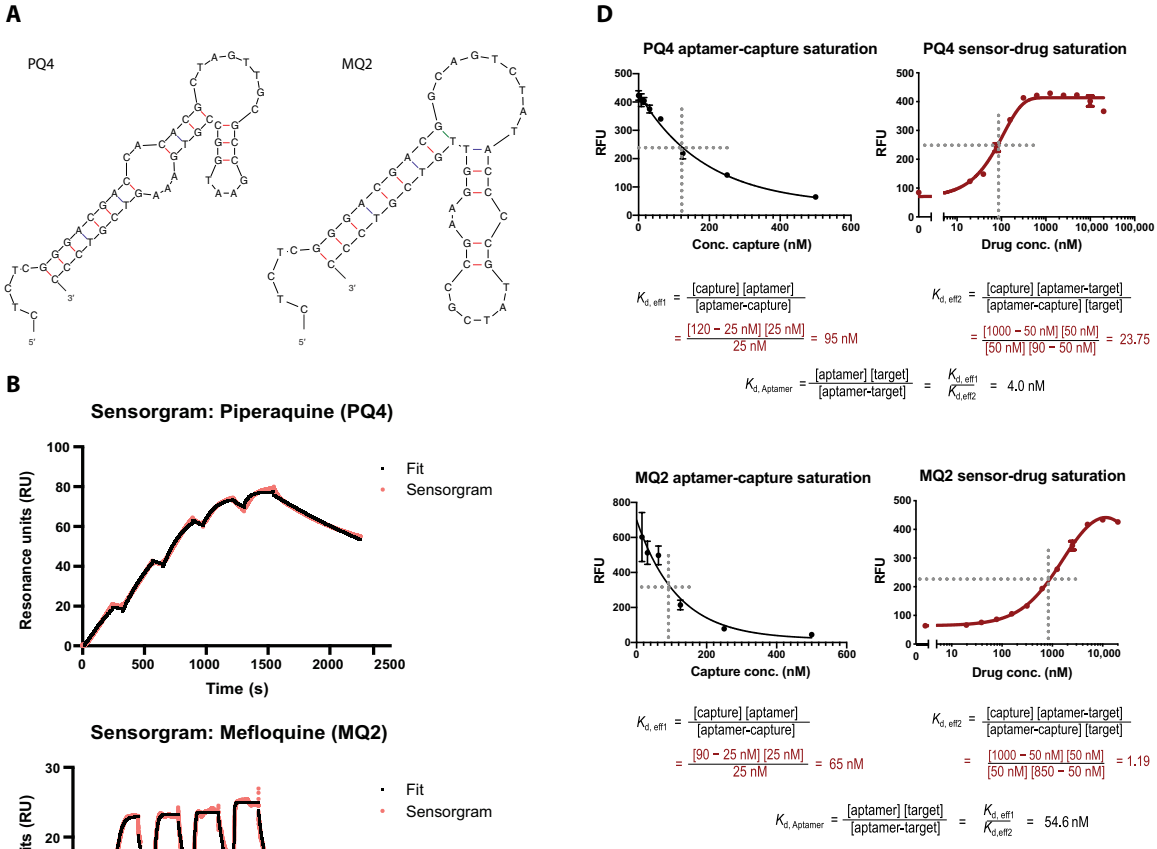
For sensor development, selected aptamer sequences were truncated to remove primer regions following a protocol previously optimized by Yang *et al.* (*26*). A small-molecule fluorophore was conjugated to the 5′ end of the aptamer and the 3′ biotin molecule of the original SELEX capture strand was replaced with a small-molecule quencher. Various fluorophore/quencher combinations were tested to enhance performance in human serum. Fluorophores were selected to reduce signal quenching and autofluorescent effects of serum components. Ultimately, an Alexa 647 fluorophore and BHQ9 quencher from Integrated DNA Technologies (IDT) were selected for the final serum sensor. Quencher molecules of several lengths were tested as well as various ratios of aptamer to quencher to optimize signal-to-noise response. Increasing quencher length or concentration inhibited the release of aptamer from quencher, increasing sensor specificity while decreasing sensitivity (fig. S3). Optimized aptamer:quencher ratios were determined to be 1:10 for the PQ4 sensor and 1:5 for the MQ2 sensor. A 13-base-long quencher oligo was selected for use in both sensors. Final sensor formulations are listed in Table 1.

Following the sensor protocol (Fig. 1E), the PQ4 and MQ2 sensor performance was evaluated in drug-spiked serum samples. The limit of detection (LOD) and limit of quantification (LOQ) for sensor PQ4 were 2 and 50 ng/ml, respectively, and those for sensor MQ2 were 8 and 325 ng/ml, respectively (Fig. 3).

For the sensors to be effective tools for tracking specific drug use, the aptamers must be capable of differentiating between similarly structured, commonly used antimalarial compounds and their metabolites. To assess sensor cross-reactivity, spiked serum samples were prepared using drug standards provided by the WorldWide Antimalarial Resistance Network (WWARN). Acetaminophen was also tested as it is commonly taken in conjunction with antimalarials.

The PQ4 sensor exhibited no cross-reactivity to similarly structured antimalarial compounds or to acetaminophen (Fig. 4A). The MQ2 sensor reported some cross-reactivity to several quinoline compounds (Fig. 4B). However, responses to amodiaquine and its active metabolite desethylamodiaquine occurred at concentrations greater than 1000 ng/ml, which is above standard clinical patient maximum concentrations (C_{max}) of both compounds (~50 and ~500 ng/ml, respectively) (*39*). The MQ2 sensor also had slight cross-reactivity

Downloaded from http://stm.sciencemag.org/ by 60259981 on March 17, 2021



C

	k_a (1/Ms)	SE (k_a)	k_d (1/s)	SE (k_d)	K_d (M)	R_{max} (RU)	X^2 (RU^2)
Piperaquine aptamer (PQ4)	2.06×10^6	1.9×10^2	5.01×10^{-4}	7.6×10^{-7}	2.43×10^{-9}	77.7	0.817
Mefloquine aptamer (MQ2)	7.64×10^5	1.1×10^4	1.47×10^{-2}	2.1×10^{-4}	1.92×10^{-8}	24.4	0.322

Fig. 2. Aptamer structures and K_d calculations. (**A**) Mfold predicted aptamer folding. (**B**) Piperaquine aptamer (PQ4) and mefloquine aptamer (MQ2) sensorgrams. Biotinylated aptamers were immobilized to neutravidin-coated CM5 chips and drug target solutions of increasing concentration were injected without regeneration. A one-site binding model was fit to the sensorgrams using single-cycle kinetic analysis. The experimental observations are reported in red and the theoretical fit is in black. Piperaquine (molecular weight: 535.51 g/mol) injection concentrations: 4.9, 9.8, 19.6, and 39.1 nM. Mefloquine (molecular weight: 378.312 g/mol) injection concentrations: 46.9, 93.8, 188, 375, and 750 nM. (**C**) Biacore characterization results. SE: standard error. (**D**) Calculations via fluorescence saturation curves. The fluorescent sensor response describes an equilibrium between aptamer-capture and aptamer-target binding. By taking this competitive binding into account, we can calculate a K_d using sensor saturation curves. A dissociation constant for the capture oligonucleotide-aptamer binding is first determined. Then, the oligonucleotide dissociation in the presence of target is measured and the two equilibrium constants obtained from these analyses are combined to give a dissociation constant for the binding of ligand with aptamer. The K_d values obtained by this method were 4.0 nM for the PQ4 aptamer and 54.6 nM for the MQ2 aptamer.

to chloroquine at concentrations above 1000 ng/ml; however, the C_{max} of chloroquine is also considerably lower, ~400 ng/ml (*40*, *41*). The chemical structure of tested compounds including target drugs, related antimalarial compounds, active metabolites, and acetaminophen are shown in Fig. 4C.

Validation against LC-MS standard drug detection method, accuracy, and precision

Next, sensor performance was validated against an LC-MS standard drug measurement method. Spiked plasma samples were prepared at the Department of Clinical Pharmacology, Mahidol Oxford Tropical Medicine Research Unit (MORU) in Bangkok, Thailand. Samples were blinded and analyzed independently via LC-MS at MORU and via aptamer sensor at the NIH Laboratory of Malaria and Vector Research, Rockville MD. The comparison of both methods is shown in Fig. 5 via scatter and Bland-Altman plots. St. Laurent correlation values of the averages of five replicates were 0.994 (95% CI: 0.969 to 0.999) for the PQ4 sensor and 0.986 (95% CI: 0.947 to 0.997) for the MQ2 sensor. All samples run on the aptamer assay were compared against the same standard curve (interpolation calculations using standard curves are detailed in Materials and Methods).

Aptamer assay performance was also assessed for inter-, intra-, and total assay variation. Five quality control (QC) samples of piperaquine- and mefloquine-spiked serum were prepared and tested

Downloaded from http://stm.sciencemag.org/ by 60259981 on March 17, 2021

Table 1. Sensor formulations. Optimal sensors for the serum platform were determined to be an Alexa 647 fluorophore–labeled aptamer with a 13-mer Iowa Black-tagged (IAB RQ) quencher molecule at an aptamer:quencher ratio of 1:5 for the PQ4 sensor and 1:10 for the MQ2 sensor. For use in crushed tablets, a fluorescein (FAM) fluorophore-tagged aptamer and 14-mer dabcyl (DAB) quencher were selected because this combination provided sufficient sensitivity for assessing drug content in tablets while reducing cross-reactivity. The tablet matrix did not have autofluorescence and quenching effects observed in serum and thus did not require the use of a higher-wavelength fluorophore. Both tablet sensors were prepared at an aptamer:quencher ratio of 1:5.

Serum sensors	
Piperaquine (PQ4)	
Aptamer	/5Alex647N/CTCTCGGGACGACCACACGCTAGTTGCGCCGAATGGCCGTGAAAGTCGTCCC
Quencher	GTCGTCCCGAGAG/3IAbRQSp/
Ratio	1:10
Mefloquine (MQ2)	
Aptamer	/5Alex647N/CTCTCGGGACGACGGCAGTCTATACCCCGTATCGCCGAAGGTTGTCGTCCC
Quencher	GTCGTCCCGAGAG/3IAbRQSp/
Ratio	1:5
Tablet sensors	
Piperaquine (PQ4)	
Aptamer	/56-FAM/CTCTCGGGACGACCACACGCTAGTTGCGCCGAATGGCCGTGAAAGTCGTCCC
Quencher	GGTCGTCCCGAGAG/3Dab/
Ratio	1:5
Mefloquine (MQ2)	
Aptamer	/56-FAM/CTCTCGGGACGACGGCAGTCTATACCCCGTATCGCCGAAGGTTGTCGTCCC
Quencher	CGTCGTCCCGAGAG/3Dab/
Ratio	1:5

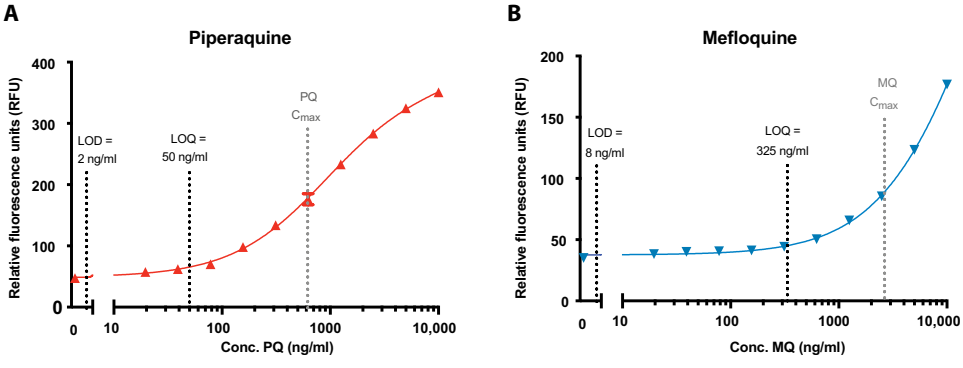


Fig. 3. Serum sensor functional ranges. Sensitivity of aptamer sensors was enhanced through fluorophore optimization. Fluorescent output is reported on the *y* axis and drug concentration of spiked serum is reported on the *x* axis. (**A**) Piperaquine serum sensor performance in spiked human serum. (**B**) Mefloquine serum sensor performance in spiked human serum. The limit of detection (LOD), calculated as average blank plus 3 times the SD of blank, and the limit of quantification (LOQ), calculated as average blank plus 10 times the SD of blank, are indicated as dotted lines. Averages of three replicates of each drug concentration are plotted, and the LOD and LOQ were calculated from 10 replicates of blanks. SD error bars are not visible when smaller than the symbol size. Sample replicates were combined with the sensor separately and compared against the same standard curve. Typical maximum serum concentrations associated with standard treatment of each drug are indicated by the gray dashed lines (*31*, *32*, *35*).

in five replicates across 4 days. Accuracy results reported less than 15% deviation from spiked values across all tested samples for both sensors. Total assay coefficients of variation (%CV) ranged from 7.29% to 38.54% (PQ4) and 8.49% to 23.82% (MQ2) from the assay LOQ through 10,000 ng/ml, with highest variance at the assay LOQ (fig. S4). In addition, potential variability in background signal from individual serum samples was assessed in blank samples from five individuals per sensor. Effects of serum matrix variability on sensor performance were determined to be minimal (fig. S5).

Piperaquine sensor validation in healthy volunteer and patient samples

Next, the piperaquine sensor was validated in plasma samples from healthy volunteers and patients with malaria. Healthy volunteers participated in an open-label study to evaluate safety, tolerability, potential pharmacokinetic interactions, and mosquito mortality of orally administered ivermectin, primaquine, and DHA-piperaquine in healthy adult participants (*42*). Patient samples were collected from a randomized controlled trial to compare the tolerability and radical curative efficacy of primaquine regimens with either chloroquine or DHA-piperaquine (*43*).

Samples were assessed via LC-MS by the MORU Department of Clinical Pharmacology. Blinded samples were shipped from MORU to the NIH, where they were assessed using the PQ4 aptamer assay. The results showed good agreement between the two methods in patient and healthy volunteer samples (Fig. 6). The Bland-Altman plot indicates that there is no substantial reporting bias between the two methods across relevant drug concentrations.

Downloaded from http://stm.sciencemag.org/ by 60259981 on March 17, 2021

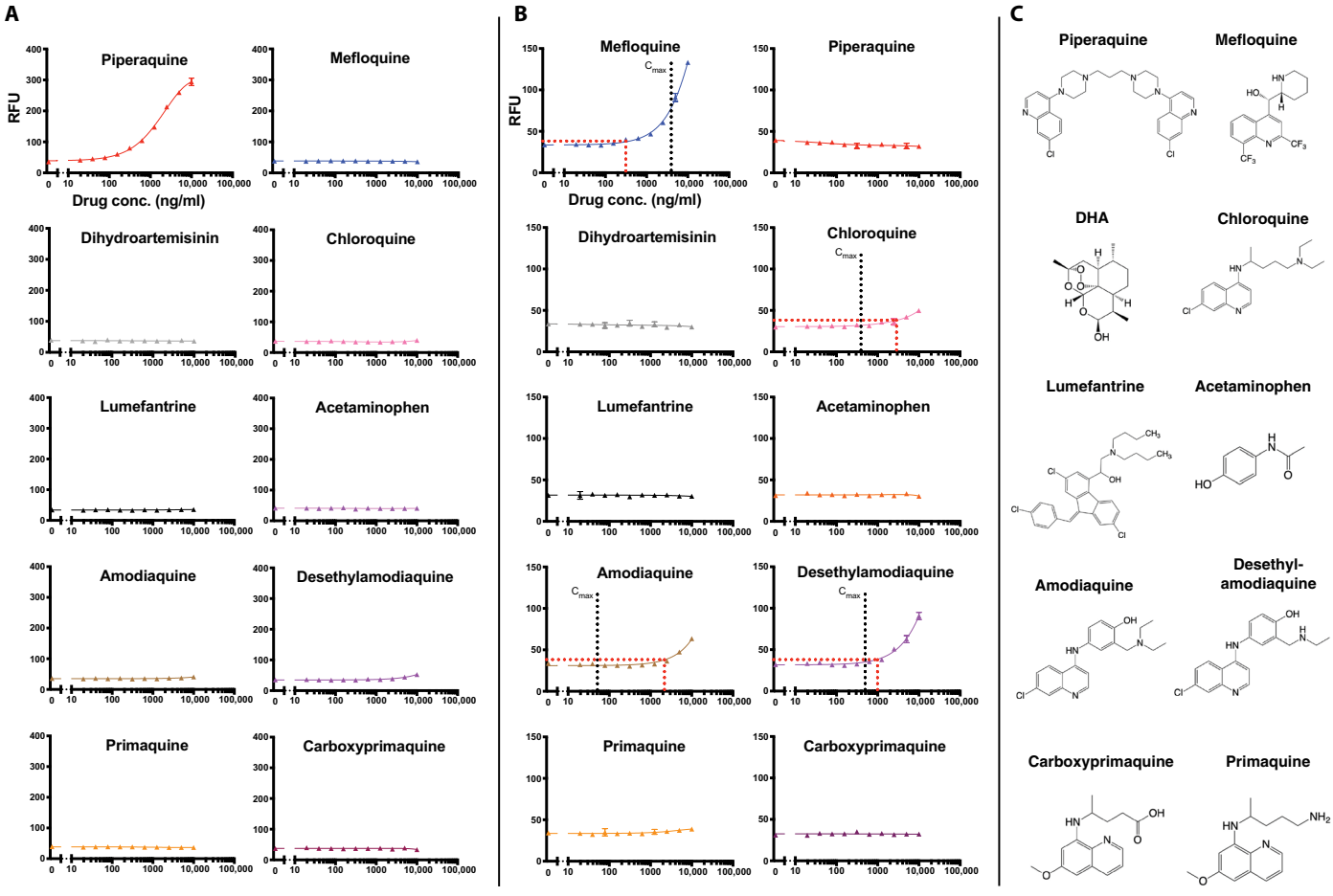


Fig. 4. Aptamer sensor cross-reactivity to similarly structured antimalarial compounds and metabolites. The aptamer sensor response to nine other antimalarial drugs or metabolites in human serum are reported for both the piperaquine and mefloquine sensors. (**A**) The PQ4 sensor response to quinoline antimalarial drugs, their active metabolites, dihydroartemisinin (DHA), or acetaminophen at relevant concentrations. (**B**) The MQ2 sensor response to the same relevant compounds. The black dotted line denotes maximum clinical concentrations of each cross-reacting compound and the red dotted line illustrates mefloquine LOQ signal on cross-reacting drug plots, showing that mefloquine LOQ signal occurs above the C_{max} of cross-reacting compounds. All conditions were tested in human serum in triplicate, the averages are plotted, and SD error bars are shown when greater than the size of the symbols. Sample replicates were combined with the sensor separately and compared against the same standard curve. (**C**) Chemical structures of the tested compounds.

Sensor modification for assessment of crushed tablets

The same isolated PQ4 and MQ2 aptamers were also optimized to function as sensors for dissolved tablets to assess drug quality. Following a similar optimization protocol as described for the serum sensors, sensor conditions were determined to be 5′-fluorescein–labeled aptamers with 14-mer dabcyl quenchers at an aptamer:quencher ratio of 1:5 for both the piperaquine and mefloquine sensor. These conditions were selected to prioritize target specificity over sensitivity. The fluorescein and dabcyl fluorophore/quencher pair was selected for the tablet sensor because the sample matrix does not require a higher wavelength readout to avoid interference. The LOD and LOQ of the tablet sensors were 50 and 61 ng/ml for piperaquine and 45 and 67 ng/ml for mefloquine, respectively; sensor selectivity is also reported in Fig. 7.

Both sensors have a similar functional range of 60 or 70 to 2500 ng/ml. For accurate quantification, high-concentration tablet preparations should be diluted to concentrations within this functional range. The piperaquine sensor showed no cross-reactivity to any of the potentially interfering drugs or excipient compounds tested; however, similar to the serum sensor, the mefloquine tablet sensor does respond to high concentrations of chloroquine and amodiaquine (Fig. 7). It seems unlikely that a counterfeit mefloquine tablet would contain more amodiaquine or chloroquine than a typical adult amodiaquine or chloroquine dose. However, if this were the case, it may not be distinguishable from a proper mefloquine-containing tablet. This is a limitation of the tablet sensor specifically as dissolutions of tablets could feasibly contain high concentrations of other compounds. Sensor development and characterization were performed using drug and excipient stocks prepared as described in Materials and Methods, and the piperaquine sensor performance was also evaluated in a dissolved expired DHA-piperaquine tablet preparation. However, because the tablet was not assessed via any other method of detection, the drug content of the tablet was not known, and this experiment only serves as a proof of principle that the sensor reports reasonable results in a crushed tablet (fig S6).

Downloaded from http://stm.sciencemag.org/ by 60259981 on March 17, 2021

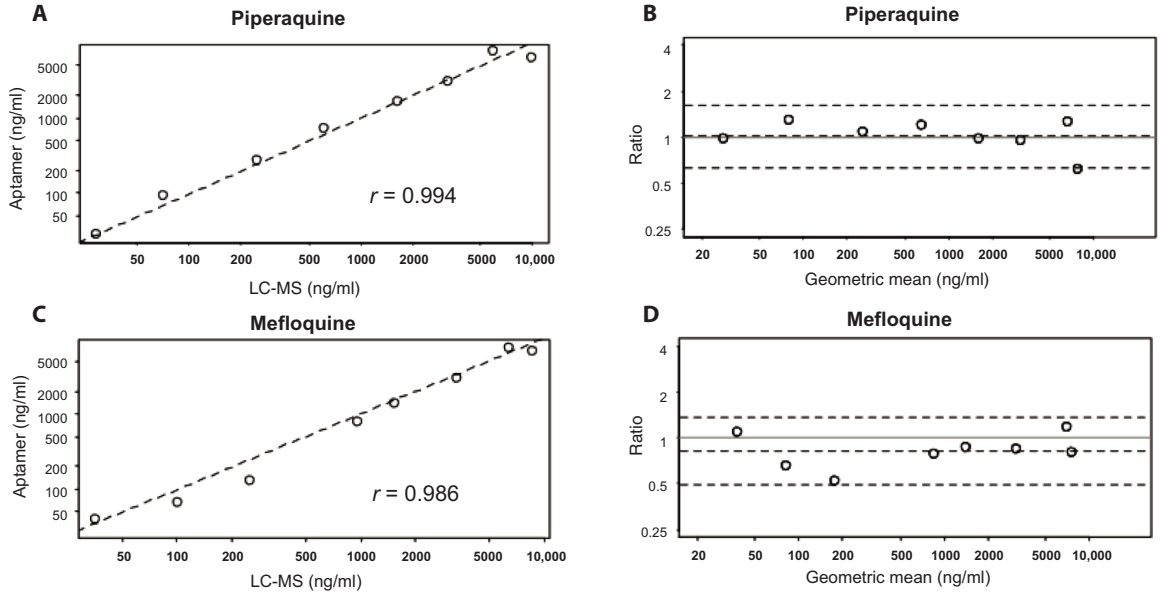


Fig. 5. Aptamer sensors compared to LC-MS standard. Blinded, spiked plasma samples (top panels: piperaquine, bottom panels: mefloquine) were analyzed using the aptamer assay at the NIH in Maryland and via LC-MS at the MORU pharmacology laboratory in Bangkok, Thailand. (**A**) and (**C**) plot the average of five aptamer measurements, the dashed line is the line of equality, and *r* is the St. Laurent correlation. (**B**) and (**D**) show Bland-Altman plots of the average values: geometric mean of aptamer and LC-MS versus ratio of aptamer over LC-MS. Dashed lines are the ratio of geometric means and 95% prediction limits, and the solid line is a reference of 1. Each replicate of a given sample was independently combined with sensor and each was then compared against the same standard curve.

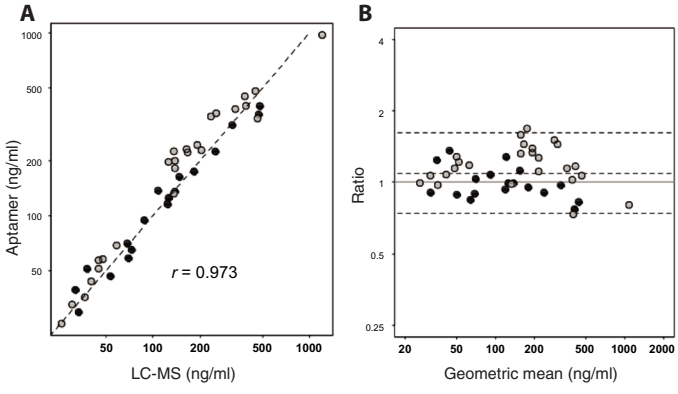


Fig. 6. Piperaquine aptamer assay validation in patient samples. Blinded patient plasma samples in the range of 20 through 1200 ng/ml were analyzed via the PQ4 aptamer assay and via LC-MS. This dataset includes a total of $n = 43$ [18 patient samples (black) and 25 healthy volunteer samples (gray)]. (**A**) The average of three aptamer sensor replicates plotted against values obtained via LC-MS standard drug detection methods. The dashed line is the line of equality and *r* is the St. Laurent correlation. For the agreement measure, the log-transformed data are used. (**B**) Bland-Altman plot of the average values: geometric mean of aptamer and LC-MS versus ratio of aptamer over LC-MS. Dashed lines are the ratio of geometric means and 95% prediction limits, and the solid line is a reference of 1. Sample replicates were combined with sensor separately and compared against the same standard curve. Participant-level data are listed in data file S1.

DISCUSSION

The ability of aptamers to differentiate between similarly structured small molecules has substantial promise for the field of drug detection research. Aptamer sensors can provide rapid, portable, and low-cost alternatives to current drug detection methods. They are inexpensive, easy to synthesize, and more stable to degradation than protein antibodies. The aptamer sensors described in this research use reagents that cost less than $0.25 per sample and only require access to a standard fluorimeter. The sensor format can be modified to function with various matrices including human samples and dissolved drug tablets. Adjusting sensor quencher length and concentration provides flexibility to fine-tune assay sensitivity and specificity depending on desired use, and the format is easily adapted to detect other small molecules.

The findings of this research could provide a new tool for researchers in malaria endemic countries to easily collect drug use and adherence data from a study population. This sensor would not replace the highly sensitive and accurate LC-MS drug detection methods required for pharmacokinetic analysis of new compounds. However, the assay could fill a current technology gap, allowing researchers to quickly and inexpensively collect data on drug use and tablet quality using standard equipment in their own laboratories. An accessible and affordable tool to detect antimalarial drug compounds from patient samples would allow researchers to monitor adherence during mass drug administration campaigns, to inform inclusion into research protocols, to assess instances of drug toxicity, to survey drug use in a region, and, in conjunction with molecular marker data, to track emerging resistance. In addition, the tablet assay provides a simple and inexpensive method to assess medicine quality—a major barrier to the regulation of medicines around the world.

This research reports exciting promise of a potentially useful assay, but several limitations of the study should be noted. First, the piperaquine aptamer assay was validated in patient samples; however, the mefloquine aptamer assay should also be tested in patient samples to continue to build confidence in the platform's performance in relevant samples. Second, we report sensitivity and specificity of the tablet assay platform here, but further validation of the tablet

Downloaded from http://stm.sciencemag.org/ by 60259981 on March 17, 2021

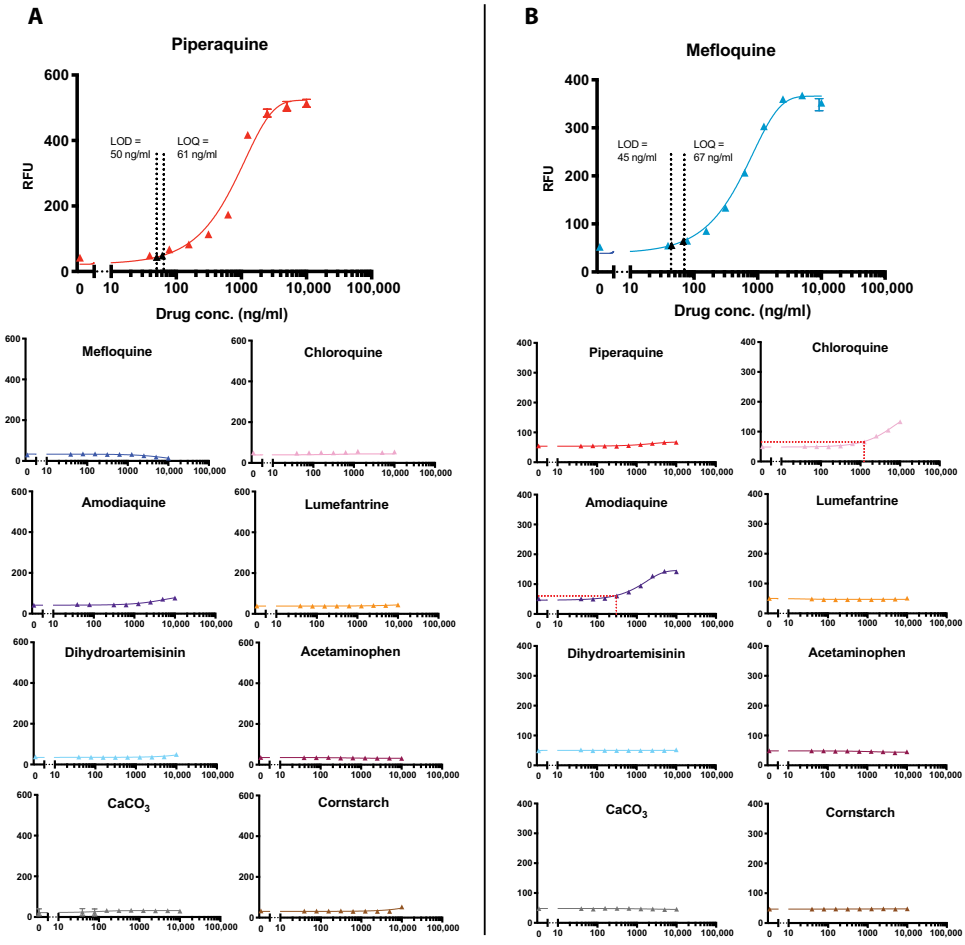


Fig. 7. Functional range and cross-reactivity of tablet sensors. The sensitivity and specificity of the adapted aptamer sensors for tablet quality testing. The LOD of each sensor, calculated as average blank plus 3 times the SD of blank, and the LOQ, calculated as average blank plus 10 times the SD of blank, are plotted here as well as cross-reactivity testing with eight similarly structured antimalarial drugs or commonly used tablet fillers or excipients. (**A**) Piperaquine tablet sensor LOD, LOQ, and specificity. The functional range of the piperaquine tablet sensor is about 60 to 2500 ng/ml, and it is highly specific with no notable cross-reactivity to any of the tested substances. (**B**) Mefloquine tablet sensor LOD, LOQ, and specificity. The functional range of the mefloquine tablet sensor is about 70 to 2500 ng/ml. The mefloquine tablet sensor shows cross-reactivity to amodiaquine and chloroquine at very high concentrations. The red lines illustrate the mefloquine LOQ signal on cross-reacting drug plots, showing the necessary concentration of cross-reacting drug to reach mefloquine LOQ signal. All drug concentrations were tested in triplicate, with replicates mixed with sensor independently and compared against the same standard curve. The LOD and LOQ were calculated from 10 blank replicates. Drug curves plot the average of three replicates with SD error bars shown when greater than the symbols.

assay against a current standard detection method for medicine quality assessment should be performed. Although, in its current format, the assay requires access to a fluorimeter, in the future, the sensor could be adapted to a colorimetric readout negating the need for lab-based equipment and a drug standard curve. The assay could be modeled after a dipstick immunoassay format and the aptamers would provide superior compound specificity over current drug-binding antibodies (*44*). An aptamer-based dipstick format would further improve access to antimalarial drug use and quality testing worldwide.

In its current format, this assay could empower local malaria researchers, enabling them to collect drug use data without having to ship frozen patient samples to an international laboratory for analysis. Expanding the library of small-molecule drug-binding aptamers could prove useful for monitoring drug use and tablet quality for other diseases as well. For example, a low-cost assay to measure plasma concentrations of tuberculosis drugs, which have challenging regimens lasting months to years, could help determine patient adherence and susceptibility for recurring or resistant infections. The exquisite sensitivity and specificity of small-molecule binding aptamers combined with the flexibility of the sensing platform highlight the promise of this technique to improve our ability to research drug use and quality and understand their impact on emerging drug resistance.

MATERIALS AND METHODS

Study design

The goal of this study was to develop and characterize a fluorescent aptamer sensor for the detection of antimalarial drugs piperaquine and mefloquine. We performed several SELEX experiments, fine-tuning selection conditions until aptamers with desired sensitivity and specificity were identified (final SELEX conditions are listed in tables S1 and S2). Aptamer sensitivity was characterized via surface plasmon resonance using a Biacore T-100, and specificity was assessed via fluorescent sensor response to similarly structured antimalarial drugs and potentially interfering compounds. The aptamer sensors were validated against standard LC-MS drug detection methods in blinded drug-spiked plasma samples prepared by the MORU pharmacology laboratory in Bangkok, Thailand. Blinded samples were shipped to the NIH where they were assessed independently via the aptamer assay. Results were unblinded after aptamer assay results were shared. The piperaquine fluorescent sensor was further validated in samples of patients with malaria (Clinicaltrials.gov: NCT01640574) and healthy volunteers (Clinicaltrials.gov: NCT02568098), which were similarly blinded and shipped from Bangkok, Thailand to the NIH for aptamer analysis and then compared with LC-MS standard results. The aptamer sensors were then adapted from a human sample platform to a drug quality platform capable of measuring drug content from dissolved tablets. Replicates were determined by sample availability and are listed in figure legends for all experiments.

Aptamer selection via capture-SELEX

All buffers were prepared according to table S3. The aptamer library, capture oligo, and primers were originally designed and optimized by Yang *et al.* (*26*).

Downloaded from http://stm.sciencemag.org/ by 60259981 on March 17, 2021

Library: GGAGGCTCTCGGGACGAC(N30)GTCGTCCCGATGCTGCAATCGTAA.
Capture oligo: 5′GTCGTCCCGAGAGCCATA-BioTEG3′.
Forward primer: 5′GGAGGCTCTCGGGACGAC3′.
Reverse primer: 5′TTACGATTGCAGCATCGGGACG3′.

The library contains a 30-mer random region flanked by conserved primer regions with a conserved capture sequence for immobilization. All oligos were synthesized by IDT (Coralville, IA). Oligo stock solutions were prepared at 100 μM in deoxyribonuclease/ribonuclease-free water and stored at −20°C. For each round of SELEX, aptamer library and capture oligo were prepared in selection buffer at a 1:5 ratio and incubated in boiling water for 5 min to allow proper annealing. To prepare the column, 250 μl of streptavidin agarose resin (Pierce Biotech catalog no. 732-6204) was added to a micro bio-spin column (Bio-Rad, catalog no. 732-6204) and washed with selection buffer. The library/capture solution was applied to the column three times by collecting the column flow-through and reapplying it to ensure sufficient immobilization.

The column was washed 10 to 24 times with 250 μl of selection buffer to remove any weakly bound sequences. After washing, negative selection steps were performed following the conditions listed in tables S1 and S2. The SELEX protocols included two sets of negative selections in later rounds; the first negative selection consisted of drug targets and the second consisted of diluted pooled human serum (Interstate Blood Bank, Inc. Memphis, TN). Each negative selection step was followed by 12 to 24 wash steps before positive selection.

For each SELEX round, three positive target elutions were performed at the concentrations described in tables S1 and S2. Each wash, positive elution, and negative elution used a volume of 250 and 5 μl of selected elutions, which were saved for the small-scale PCR described later. Each of the three positive selection elutions were collected and combined. This volume was added to a 10-kDa molecular weight cutoff column (EMD Millipore, catalog no. UFC5003) and concentrated following the manufacturer's protocol, reloading and repeating until all 750 μl were added and reduced to roughly 100 μl. To wash the concentrated DNA, 400 μl of deionized water was added to the column and the volume was again reduced to 100 μl.

The concentrated positive elution sample was amplified using a 5′ biotinylated reverse primer (Takara Taq Premix). The library was gradually amplified (4 to 6 cycles at a time) and run on a 3% agarose, 0.02% ethidium bromide gel until bands were visible. Optimized PCR conditions were as follows: (i) 95°C for 2 min, (ii) 95°C for 15 s, (iii) 59°C for 30 s, (iv) 72°C for 45 s, and (v) 72°C for 2 min, repeating steps (ii) to (iv). A small-scale PCR was also run each round to generate an elution profile to track SELEX progress using 5 μl of the initial library, first and last washes, negative elutions, and positive elutions saved during selection. The small-scale PCR was analyzed to determine SELEX progress after each round to inform adjustments to subsequent selection conditions. In later rounds, comparatively less DNA eluted during wash and negative selection steps whereas more eluted during positive selection, showing the evolution of the library toward positive target specificity (Fig. 1B).

After amplification, the library was purified and concentrated with a 10-kDa molecular weight cutoff column, resuspended in single-stranded buffer (table S3), and loaded onto a fresh streptavidin agarose column. The immobilized dsDNA library was incubated for 10 min in 0.2 N NaOH to release the nonbiotinylated strands, which were collected, neutralized with HCl and 2X selection buffer, and quantified via Nanodrop (Denovix DS-11 FX+). One hundred picomoles of the library was carried forward to the next SELEX round.

Sequencing and analysis of final SELEX pool

Positive selection elutions from final SELEX rounds were amplified and concentrated via ethanol precipitation. Cloning and transformation were performed using the TOPO TA Cloning Kit (Invitrogen catalog no. 45-0641). Colonies (25 to 30) were amplified and run on a 3% agarose, 0.02% ethidium bromide gel to screen for positive inserts. Positive samples were purified using an ExoSAP-IT kit from Applied Biosystems (catalog no. 78200) and Sanger sequenced by Eurofins Scientific (Louisville, KY). M13 primers were used for sequencing to ensure quality sequencing of the entire library, including library primers. Results were sorted based on sequence enrichment and folding structure as hypothesized by Mfold. Mfold conditions were set to 137 mM Na^+, 2 mM Mg^{2+}, and 20°C, with no constraints.

Four to six sequences were selected and analyzed via a single round of sequence-specific SELEX following the previously described protocol to produce a sequence-specific elution profile. This generated an elution profile describing the relative amount of DNA eluted during wash, negative, and positive selection steps for each sequence of interest. These specific elution profiles were analyzed to select the most promising sequences for sensor development. Selected sequences from the most promising piperaquine and mefloquine SELEX experiments, their Mfold predicted structure, and their specific elution profiles are shown in fig. S7.

Affinity measurements via Biacore

Surface plasmon resonance (Biacore T-100) was used to analyze the interaction between aptamers and drug targets. Neutravidin was immobilized on a CM5 surface using amine coupling methodology. In one flow cell, biotinylated drug-selected aptamers were injected over the surface until a quantity of 1200 to 1500 resonance units (RU) was immobilized. On a second surface, a biotinylated random aptamer library was immobilized similarly and served as a binding control. After conditioning the surfaces using injections of 50 mM NaOH, binding was measured by single-cycle injection of increasing concentrations of the drug target. Selection buffer (table S3) was used as a running buffer for all experiments. The results were analyzed by global fitting of the data to a 1:1 Langmuir kinetic model using the Biacore evaluation software.

Sensor design

Aptamer sequences of interest were synthesized and labeled with 5′ fluorophores by IDT. Capture sequences of 13- and 14-mer lengths were synthesized and tagged with 3′ quencher molecules. Various small-molecule fluorophores, quenchers, quencher oligo lengths, and quencher oligo concentrations were evaluated to determine optimal sensor preparations for both serum and tablet sample matrices. The fluorophore-tagged aptamer sensors were prepared in selection buffer at a concentration of 100 nM. Quencher tagged capture sequences (13 and 14 mer) now referred to as quencher molecules were prepared at either 500 nM (1:5) or 1 μM (1:10) concentrations in selection buffer. As shown in fig. S3, sensor specificity and sensitivity can be adjusted by varying the length and amount of quencher oligo in the final sensor solution. Optimized sensor formulations are shown in Table 1.

Downloaded from http://stm.sciencemag.org/ by 60259981 on March 17, 2021

Aptamer and quencher solutions were combined at prescribed concentrations, incubated in boiling water for 5 min, and then cooled at room temperature to ensure proper annealing. The resulting sensor solution was combined 1:1 with sample (40 μl sensor + 40 μl sample). After 30 min of equilibration, the sample was transferred (75 μl) to a Corning black flat bottom 384-well plate (catalog no. 3577) and read by a Molecular Devices Spectramax 190 microplate reader at corresponding excitation/emission wavelengths (ex/em) (FAM: 485/535, Alexa 647: 645/665). Each replicate refers to an independent combination of sensor stock and sample.

Aptamer sensor validation against LC-MS and in human plasma samples

The accuracy of the aptamer sensors was validated against a reference LC-MS method for drug detection. Plasma samples spiked with piperaquine or mefloquine were prepared and analyzed via LC-MS at MORU in Bangkok, Thailand and shipped to the NIH for independent analysis with the aptamer sensor. The samples were blinded during aptamer sensor analysis and results were compared to LC-MS values. For aptamer sensor analysis, plasma samples were diluted 1:5 in selection buffer and then each replicate was combined 1:1 (40 μl sample + 40 μl sensor) with sensor solution (prepared as described in Table 1). After 30 min of equilibration, each replicate was transferred (75 μl) to a Corning black flat bottom 384-well plate and read at ex/em: 645/665. A standard curve of each drug (prepared in plasma and diluted 1:5 in selection buffer) was run with the samples for drug concentration interpolation.

Following the same protocol, plasma samples from healthy volunteers and patients with malaria were assessed for piperaquine concentration via LC-MS by the MORU pharmacology laboratory, blinded, and shipped to LMVR, Rockville, MD. The samples were assessed using the piperaquine aptamer sensor and concentrations were interpolated from a piperaquine standard curve.

LC-MS protocol

Concentrations of piperaquine and mefloquine were measured using methods validated according to U.S. Food and Drug Administration guidelines (*12*, *45*). Drug quantification was performed in a quality-controlled setting using liquid chromatography coupled with tandem mass spectrometry. In brief, plasma sample extraction was performed in a 96-well format using MPC-SD SPE plates (3M, Eagan, MN, USA) for piperaquine and Phree phospholipids removal plates (Phenomenex, Torrance, CA, USA) for mefloquine. Stable isotope-labeled internal standards were used to compensate for potential recovery and matrix effects. The extracted drugs were separated using a Dionex Ultimate 3000 UHPLC (Thermo Fisher Scientific, Waltham, MA, USA) equipped with a Gemini C_{18} column (Phenomenex) for piperaquine and a Zorbax SB-CN (Agilent, Santa Clara, CA, USA) for mefloquine. An API5000 triple-quadrupole mass spectrometer and Analyst 1.7 software (AB Sciex, Framingham, MA, USA) were used for drug detection and quantification. The coefficient of variation for the QC samples was within the set limits and did not exceed 10% for any QC sample. The lower limits of quantification were 9.55 ng/ml for mefloquine and 1.5 ng/ml for piperaquine.

Characterizing sensor batch variability and response to serum sample variation

QC samples were prepared in pooled human serum at five different concentrations: at the assay LOQ, above the range of sensor function (Hi), and three values within the sensor functional range (QC1 to QC3). QC samples were frozen, and each sample was tested in five replicates over 4 days; each day, a new sensor solution was prepared. The inter-, intra-, and total assay variability were evaluated via coefficient of variation analysis. To assess the background effects of varying serum samples, samples from 10 different individuals (Interstate Blood Bank, Memphis, TN) were tested against the piperaquine or mefloquine sensor. Serum samples were diluted 1:5 in selection buffer and five samples were run on each sensor in triplicate.

Cross-reactivity testing

To assess cross-reactivity, the PQ4 and MQ2 sensor responses to potentially cross-reactive compounds including commonly used antimalarial drugs, their metabolites, acetaminophen, and for the tablet sensor, compounds expected to be found in genuine or falsified antimalarial tablets such as calcium carbonate and cornstarch, were monitored. Stock solutions of these compounds were prepared according to table S4. The sensors were prepared as previously described, and the cross-reactivity curves are shown in Results (Fig. 4 and 7).

Tablet sensor characterization

To assess the functional range of both the PQ4 and MQ2 tablet sensors, standard curves of piperaquine and mefloquine were prepared in selection buffer. Sensor solutions of PQ4 and MQ2 (Table 1) were heated in boiling water for 5 min, cooled to room temperature, and combined 1:1 with the drug dilutions (40 μl sensor + 40 μl sample). After 30 min of equilibration, the sample was transferred (75 μl) to a Corning black flat bottom 384-well plate and read at ex/em: 485/538.

To confirm that the aptamer sensors can detect desired compounds from crushed tablets, an expired Eurartesim tablet (40 mg DHA/320 mg piperaquine tetraphosphate; Sigma-Tau, Rome, Italy, batch no. 150728, mfg. date: June 2015, exp. date: May 2017) was obtained and tested in March 2019. The tablet was dissolved following a previously published protocol for tablet quality testing (*46*). The tablet was crushed using a mortar and pestle, transferred to a large volume flask, and then dissolved in water, 2.5% MeOH, and 12.5 μM HCl to a piperaquine concentration of 0.5 mg/ml. Because of the presence of insoluble tablet components, the dissolved tablet solution was nonhomogeneous with visible precipitates. An aliquot of the supernatant was collected, centrifuged to remove precipitates, and this stock was then further diluted to prepare a standard curve of predicted piperaquine concentration ranging from 5000 to 20 ng/ml. This was run against a laboratory-prepared piperaquine standard curve to assess piperaquine content. Results are shown in fig. S6.

Interpolation using standardized curves

The standardized curves were fit using least squares regression with a one-phase exponential model, where the RFU value, Y (vertical axis), is predicted as a function of the concentration, X (horizontal axis), by the following equation

$$Y = Y_{max} + (Y_{null} - Y_{max}) \times \exp(-K \times X) + \varepsilon$$

where Y_{null} represents the background RFU, K is the concentration scaling factor, Y_{max} is the estimated maximum RFU value at an infinite concentration, and ε is the error term assumed normally

Downloaded from http://stm.sciencemag.org/ by 60259981 on March 17, 2021

distributed with mean 0. Samples were run in three or five replicates determined by availability of sample material. The mean RFU replicates is set to Y, and the concentration is the solution of the equation (or is set to 0 if $Y < Y_0$, or is set to "above the limit of detection" if $Y > Y_{max}$). Fits were done in Prism version 7 or R 3.6.3.

Statistical methods

Statistical analysis was performed in GraphPad Prism 7 and R 3.6.3. To measure agreement of the average of five replicates using the aptamer assay with the gold standard (LC-MS), we use the St. Laurent correlation after transforming the average aptamer and LC-MS concentrations to the log scale (*47*). We use Bland-Altman plots on the log-transformed values, so that each point is the geometric mean of the two assays on the x axis and the ratio of the two assays (aptamer over LC-MS) on the y axis, and the horizontal lines are the geometric means of the ratios with the 95% prediction intervals (*48*). Accuracy and precision and matrix effects results were assessed via %CV of inter-, intra-, and total assay variability (fig S4 and S5). Individual participant-level data are provided in data file S1.

SUPPLEMENTARY MATERIALS

stm.sciencemag.org/cgi/content/full/13/585/eabe1535/DC1
Fig. S1. MQ2 aptamer alternative Mfold 2D folding predictions.
Fig. S2. Supplemental Biacore experiments.
Fig. S3. Effect of quencher oligo length and concentration on sensor function.
Fig. S4. Accuracy and precision data.
Fig. S5. Serum matrix effects.
Fig. S6. Test of aptamer assay with an expired DHA-piperaquine tablet.
Fig. S7. Selection of aptamer sequences for sensor development.
Table S1. Selection protocol of a successful piperaquine SELEX experiment.
Table S2. Selection protocol of a successful mefloquine SELEX experiment.
Table S3. Buffer recipes for SELEX protocol and aptamer sensor preparation.
Table S4. Stock solutions of compounds for testing sensor cross-reactivity.
Data file S1. Individual participant-level data.

View/request a protocol for this paper from *Bio-protocol*.

REFERENCES AND NOTES

1. World Health Organization, *World Malaria Report 2019* (Geneva, 2019); https://www.who.int/publications-detail/world-malaria-report-2019.
2. World Health Organization, *World Malaria Report 2020* (Geneva, 2020); https://www.who.int/publications/i/item/9789240015791.
3. B. Hanboonkunupakarn, N. J. White, The threat of antimalarial drug resistance. *Trop. Dis. Travel Med. Vaccines* **2**, 10 (2015).
4. R. Leang, A. Barrette, D. M. Bouth, D. Menard, R. Abdur, S. Duong, P. Ringwald, Efficacy of dihydroartemisinin-piperaquine for treatment of uncomplicated *Plasmodium falciparum* and *Plasmodium vivax* in Cambodia, 2008 to 2010. *Antimicrob. Agents Chemother.* **57**, 818–826 (2013).
5. R. Leang, W. R. J. Taylor, D. M. Bouth, L. Song, J. Tarning, M. C. Char, S. Kim, B. Witkowski, V. Duru, A. Domergue, N. Khim, P. Ringwald, D. Menard, Evidence of *Plasmodium falciparum* malaria multidrug resistance to artemisinin and piperaquine in western Cambodia: Dihydroartemisinin-piperaquine open-label multicenter clinical assessment. *Antimicrob. Agents Chemother.* **59**, 4719–4726 (2015).
6. C. Amaratunga, P. Lim, S. Suon, S. Sreng, S. Mao, C. Sopha, B. Sam, D. Dek, V. Try, R. Amato, D. Blessborn, L. Song, G. S. Tullo, M. P. Fay, J. M. Anderson, J. Tarning, R. M. Fairhurst, Dihydroartemisinin–piperaquine resistance in *Plasmodium falciparum* malaria in Cambodia: A multisite prospective cohort study. *Lancet Infect. Dis.* **16**, 357–365 (2016).
7. C. J. Woodrow, N. J. White, The clinical impact of artemisinin resistance in Southeast Asia and the potential for future spread. *FEMS Microbiol. Rev.* **41**, 34–48 (2017).
8. E. A. Ashley, M. Dhorda, R. M. Fairhurst, C. Amaratunga, P. Lim, S. Suon, S. Sreng, J. M. Anderson, S. Mao, B. Sam, C. Sopha, C. M. Chuor, C. Nguon, S. Sovannaroth, S. Pukrittayakamee, P. Jittamala, K. Chotivanich, K. Chutasmit, C. Suchatsoonthorn, R. Runcharoen, T. T. Hien, N. T. Thuy-Nhien, N. V. Thanh, N. H. Phu, Y. Htut, K.-T. Han, K. H. Aye, O. A. Mokuolu, R. R. Olaosebikan, O. O. Folaranmi, M. Mayxay, M. Khanthavong, B. Hongvanthong, P. N. Newton, M. A. Onyamboko, C. I. Fanello, A. K. Tshefu, N. Mishra, N. Valecha, A. P. Phyo, F. Nosten, P. Yi, R. Tripura, S. Borrmann, M. Bashraheil, J. Peshu, M. A. Faiz, A. Ghose, M. A. Hossain, R. Samad, M. R. Rahman, M. M. Hasan, A. Islam, O. Miotto, R. Amato, B. MacInnis, J. Stalker, D. P. Kwiatkowski, Z. Bozdech, A. Jeeyapant, P. Y. Cheah, T. Sakulthaew, J. Chalk, B. Intharabut, K. Silamut, S. J. Lee, B. Vihokhern, C. Kunasol, M. Imwong, J. Tarning, W. J. Taylor, S. Yeung, C. J. Woodrow, J. A. Flegg, D. Das, J. Smith, M. Venkatesan, C. V. Plowe, K. Stepniewska, P. J. Guerin, A. M. Dondorp, N. P. Day, N. J. White; Tracking Resistance to Artemisinin Collaboration (TRAC), Spread of artemisinin resistance in *Plasmodium falciparum* malaria. *N. Engl. J. Med.* **371**, 411–423 (2014).
9. T. Mita, M. Venkatesan, J. Ohashi, R. Culleton, N. Takahashi, T. Tsukahara, M. Ndounga, L. Dysoley, H. Endo, F. Hombhanje, M. U. Ferreira, C. V. Plowe, K. Tanabe, Limited geographical origin and global spread of sulfadoxine-resistant dhps alleles in plasmodium falciparum populations. *J. Infect. Dis.* **204**, 1980–1988 (2011).
10. C. Roper, R. Pearce, S. Nair, B. Sharp, F. Nosten, T. Anderson, Intercontinental spread of pyrimethamine-resistant malaria. *Science* **305**, 1124 (2004).
11. C. J. Murray, L. C. Rosenfeld, S. S. Lim, K. G. Andrews, K. J. Foreman, D. Haring, N. Fullman, M. Naghavi, R. Lozano, A. D. Lopez, Global malaria mortality between 1980 and 2010: A systematic analysis. *Lancet* **379**, 413–431 (2012).
12. N. Lindegardh, A. Annerberg, N. J. White, N. P. J. Day, Development and validation of a liquid chromatographic-tandem mass spectrometric method for determination of piperaquine in plasma. *J. Chromatogr. B* **862**, 227–236 (2007).
13. A. V. Silva, N. Mwebaza, M. Ntale, L. L. Gustafsson, A. Pohanka, A fast and sensitive method for quantifying lumefantrine and desbutyl-lumefantrine using LC-MS/MS. *J. Chromatogr. B Analyt. Technol. Biomed. Life Sci.* **1004**, 60–66 (2015).
14. X. Chen, P. Deng, X. Dai, D. Zhong, Simultaneous determination of amodiaquine and its active metabolite in human blood by ion-pair liquid chromatography-tandem mass spectrometry. *J. Chromatogr. B Analyt. Technol. Biomed. Life Sci.* **860**, 18–25 (2007).
15. M. J. Hilhorst, G. Hendriks, R. de Vries, V. Hillewaert, T. Verhaege, N. C. Van de Merbel, A high-performance liquid chromatography-tandem mass spectrometry method for the determination of artemether and dihydroartemisinin in human plasma. *J. Chromatogr. B Analyt. Technol. Biomed. Life Sci.* **965**, 45–53 (2014).
16. L. Wiesner, K. Govender, S. A. Meredith, J. Norman, P. J. Smith, A liquid-liquid LC/MS/MS assay for the determination of artemether and DHA in malaria patient samples. *J. Pharm. Biomed. Anal.* **55**, 373–378 (2011).
17. E. M. Hodel, B. Zanolari, T. Mercier, J. Biollaz, J. Keiser, P. Olliaro, B. Genton, L. A. Decosterd, A single LC-tandem mass spectrometry method for the simultaneous determination of 14 antimalarial drugs and their metabolites in human plasma. *J. Chromatogr. B* **877**, 867–886 (2009).
18. J. Gallay, S. Prod'hom, T. Mercier, C. Bardinet, D. Spaggiari, E. Pothin, T. Buclin, B. Genton, L. A. Decosterd, LC–MS/MS method for the simultaneous analysis of seven antimalarials and two active metabolites in dried blood spots for applications in field trials: Analytical and clinical validation. *J. Pharm. Biomed. Anal.* **154**, 263–277 (2018).
19. D. Blessborn, S. Romsing, Y. Bergqvist, N. Lindegardh, Assay for screening for six antimalarial drugs and one metabolite using dried blood spot sampling, sequential extraction and ion-trap detection. *Bioanalysis* **2**, 1839–1847 (2010).
20. M. McKeague, M. C. DeRosa, Challenges and opportunities for small molecule aptamer development. *J. Nucleic Acids* **2012**, 748913 (2012).
21. R. D. Jenison, S. C. Gill, A. Pardi, B. Polisky, High-resolution molecular discrimination by RNA. *Science* **263**, 1425–1429 (1994).
22. A. D. Ellington, J. W. Szostak, In vitro selection of RNA molecules that bind specific ligands. *Nature* **346**, 818–822 (1990).
23. C. Tuerk, L. Gold, Systematic evolution of ligands by exponential enrichment: RNA ligands to bacteriophage T4 DNA polymerase. *Science* **249**, 505–510 (1990).
24. M. Mascini, *Aptamers in Bioanalysis* (John Wiley & Sons, 2008).
25. R. Nutiu, Y. Li, Structure-switching signaling aptamers. *J. Am. Chem. Soc.* **125**, 4771–4778 (2003).
26. K. A. Yang, R. Pei, M. N. Stojanovic, In vitro selection and amplification protocols for isolation of aptameric sensors for small molecules. *Methods* **106**, 58–65 (2016).
27. K.-A. Yang, M. Barbu, M. Halim, P. Pallavi, B. Kim, D. M. Kolpashchikov, S. Pecic, S. Taylor, T. S. Worgall, M. N. Stojanovic, Recognition and sensing of low-epitope targets via ternary complexes with oligonucleotides and synthetic receptors. *Nat. Chem.* **6**, 1003–1008 (2014).
28. K. M. Cheung, K. A. Yang, N. Nakatsuka, C. Zhao, M. Ye, M. E. Jung, H. Yang, P. S. Weiss, M. N. Stojanović, A. M. Andrews, Phenylalanine monitoring via aptamer-field-effect transistor sensors. *ACS Sens.* **4**, 3308–3317 (2019).
29. P. Dauphin-Ducharme, K. Yang, N. Arroyo-Currás, K. L. Ploense, Y. Zhang, J. Gerson, M. Kurnik, T. E. Kippin, M. N. Stojanovic, K. W. Plaxco, Electrochemical aptamer-based sensors for improved therapeutic drug monitoring and high-precision, feedback-controlled drug delivery. *ACS Sens.* **4**, 2832–2837 (2019).
30. J. Tarning, I. Zongo, F. A. Somé, N. Rouamba, S. Parikh, P. J. Rosenthal, W. Hanpithakpong, N. Jongrak, N. P. J. Day, N. J. White, F. Nosten, J. B. Ouedraogo, N. Lindegardh, Population pharmacokinetics and pharmacodynamics of piperaquine in children with uncomplicated falciparum malaria. *Clin. Pharmacol. Ther.* **91**, 497–505 (2012).

Downloaded from http://stm.sciencemag.org/ by 60259981 on March 17, 2021

31. J. Tarning, M. J. Rijken, R. McGready, A. P. Phyo, W. Hanpithakpong, N. P. J. Day, N. J. White, F. Nosten, N. Lindegardh, Population pharmacokinetics of dihydroartemisinin and piperaquine in pregnant and nonpregnant women with uncomplicated malaria. *Antimicrob. Agents Chemother.* **56**, 1997–2007 (2012).
32. R. M. Hoglund, L. Workman, M. D. Edstein, N. X. Thanh, N. N. Quang, I. Zongo, J. B. Ouedraogo, S. Borrmann, L. Mwai, C. Nsanzabana, R. N. Price, P. Dahal, N. C. Sambol, S. Parikh, F. Nosten, E. A. Ashley, A. P. Phyo, K. M. Lwin, R. McGready, N. P. J. Day, P. J. Guerin, N. J. White, K. I. Barnes, J. Tarning, Population pharmacokinetic properties of piperaquine in falciparum malaria: An individual participant data meta-analysis. *PLOS Med.* **14**, e1002212 (2017).
33. M. Green, K. Otieno, A. Katana, L. Slutsker, S. Kariuki, P. Ouma, R. González, C. Menendez, F. Ter Kuile, M. Desai, Pharmacokinetics of mefloquine and its effect on sulfamethoxazole and trimethoprim steady-state blood levels in intermittent preventive treatment (IPTp) of pregnant HIV-infected women in Kenya. *Malar. J.* **15**, 7 (2016).
34. M. V. D. Ferreira, J. L. F. Vieira, E. D. Almeida, J. G. B. Rivera, M. S. M. Gomes, A. M. De Siqueira, Pharmacokinetics of mefloquine administered with artesunate in patients with uncomplicated falciparum malaria from the Brazilian Amazon basin. *Malar. J.* **17**, 268 (2018).
35. E. M. Staehli Hodel, M. Guidi, B. Zanolari, T. Mercier, S. Duong, A. M. Kabanywanyi, F. Ariey, T. Buclin, H. P. Beck, L. A. Decosterd, P. Olliaro, B. Genton, C. Csajka, Population pharmacokinetics of mefloquine, piperaquine and artemether-lumefantrine in Cambodian and Tanzanian malaria patients. *Malar. J.* **12**, 235 (2013).
36. F. Corpet, Multiple sequence alignment with hierarchical clustering. *Nucleic Acids Res.* **16**, 10881–10890 (1988).
37. M. Zuker, Mfold web server for nucleic acid folding and hybridization prediction. *Nucleic Acids Res.* **31**, 3406–3415 (2003).
38. J. Hu, C. J. Easley, A simple and rapid approach for measurement of dissociation constants of DNA aptamers against proteins and small molecules via automated microchip electrophoresis. *Analyst* **136**, 3461–3468 (2011).
39. A. M. Ali, M. A. Penny, T. A. Smith, L. Workman, P. Sasi, G. O. Adjei, F. Aweeka, J. R. Kiechel, V. Jullien, M. J. Rijken, R. McGready, J. Mwesigwa, K. Kristensen, K. Stepniewska, J. Tarning, K. I. Barnes, P. Denti, Population pharmacokinetics of the antimalarial amodiaquine: A pooled analysis to optimize dosing. *Antimicrob. Agents Chemother.* **62**, e02193-17 (2018).
40. P. Kadam, N. Gogtay, S. Karande, V. Shah, U. Thatte, Evaluation of pharmacokinetics of single-dose chloroquine in malnourished children with malaria—A comparative study with normally nourished children. *Indian J. Pharmacol.* **48**, 498–502 (2016).
41. D. G. Bustos, J. E. Lazaro, F. Gay, A. Pottier, C. J. Laracas, B. Traore, B. Diquet, Pharmacokinetics of sequential and simultaneous treatment with the combination chloroquine and sulfadoxine-pyrimethamine in acute uncomplicated *Plasmodium falciparum* malaria in the Philippines. *Trop. Med. Int. Health* **7**, 584–591 (2002).
42. K. C. Kobylinski, P. Jittamala, B. Hanboonkunupakarn, S. Pukrittayakamee, K. Pantuwatana, S. Phasomkusolsil, S. A. Davidson, M. Winterberg, R. M. Hoglund, M. Mukaka, R. W. van der Pluijm, A. Dondorp, N. P. J. Day, N. J. White, J. Tarning, Safety, pharmacokinetics, and mosquito-lethal effects of ivermectin in combination with dihydroartemisinin-piperaquine and primaquine in healthy adult Thai subjects. *Clin. Pharmacol. Ther.* **107**, 1221–1230 (2020).
43. C. S. Chu, A. P. Phyo, C. Turner, H. H. Win, N. P. Poe, W. Yotyingaphiram, S. Thinraow, P. Wilairisak, R. Raksapraidee, V. I. Carrara, M. K. Paw, J. Wiladphaingern, S. Proux, G. Bancone, K. Sriprawat, S. J. Lee, A. Jeeyapant, J. Watson, J. Tarning, M. Imwong, F. Nosten, N. J. White, Chloroquine versus dihydroartemisinin-piperaquine with standard high-dose primaquine given either for 7 days or 14 days in *Plasmodium vivax* malaria. *Clin. Infect. Dis.* **68**, 1311–1319 (2019).
44. X. Ning, G. Tan, X. Chen, M. Wang, B. Wang, L. Cui, Development of a lateral flow dipstick for simultaneous and semi-quantitative analysis of dihydroartemisinin and piperaquine in an artemisinin combination therapy. *Drug Test. Anal.* **11**, 1444–1452 (2019).
45. FDA, *Bioanalytical Method Validation Guidance* (Rockville, 2001).
46. E. Maria Hodel, H. Kaur, D. J. Terlouw, Stability of dihydroartemisinin-piperaquine tablet halves during prolonged storage under tropical conditions. *Am. J. Trop. Med. Hyg.* **96**, 338–340 (2017).
47. R. T. St. Laurent, Evaluating agreement with a gold standard in method comparison studies. *Biometrics* **54**, 537 (1998).
48. J. M. Bland, D. G. Altman, Measuring agreement in method comparison studies. *Stat. Methods Med. Res.* **8**, 135–160 (1999).

Acknowledgments: We thank K. Miura for helpful comments during experimental design and manuscript editing. We thank C. Amaratunga for support throughout the project. We thank M. Stojanovic and his laboratory for SELEX protocol guidance. We thank D. Blessborn for preparing and sending spiked samples from MORU and K. Lane for cloning protocol advice. We thank R. Fairhurst for initial discussions regarding assay design. We thank P. Jittamala and C. Chu for sample collection and the healthy volunteers and patients whose samples allowed for assay validation. **Funding:** This work was supported by the Division of Intramural Research, National Institute of Allergy and Infectious Diseases (NIAID), National Institutes of Health (NIH), USA. **Author contributions:** E.S.C. performed experimental design, data collection, and manuscript writing. K.-A.Y. contributed to experimental design. K.-A.Y. and S.P. advised SELEX experiments. M.D.V. supported experiment planning and data collection. J.F.A. performed Biacore experiments. M.P.F. led statistical analysis. J.T. contributed to LC-MS analysis. T.E.W., C.A.L., and J.T. contributed to experimental design and manuscript writing. **Competing interests:** The authors declare that they have no competing interests. **Data and materials availability:** All data associated with this study are present in the paper or the Supplementary Materials.

Submitted 3 August 2020
Accepted 22 February 2021
Published 17 March 2021
10.1126/scitranslmed.abe1535

Citation: E. S. Coonahan, K.-A. Yang, S. Pecic, M. De Vos, T. E. Wellems, M. P. Fay, J. F. Andersen, J. Tarning, C. A. Long, Structure-switching aptamer sensors for the specific detection of piperaquine and mefloquine. *Sci. Transl. Med.* **13**, eabe1535 (2021).

Downloaded from http://stm.sciencemag.org/ by 60259981 on March 17, 2021

Science Translational Medicine

Structure-switching aptamer sensors for the specific detection of piperaquine and mefloquine

Erin S. Coonahan, Kyung-Ae Yang, Stevan Pecic, Maarten De Vos, Thomas E. Wellems, Michael P. Fay, John F. Andersen, Joel Tarning and Carole A. Long

Sci Transl Med **13**, eabe1535.
DOI: 10.1126/scitranslmed.abe1535

Diligent drug detection

Plasmodium falciparum resistance to slow-clearing artemisinin-based combination therapies is an emerging problem in the fight against malaria. Rather than relying on liquid chromatography–mass spectrometry, Coonahan *et al.* developed a rapid method using aptamer sensors to detect antimalarial compounds in human blood samples and crushed tablets. Aptamers specific to two antimalarial drugs, piperaquine and mefloquine, were selected and used to develop fluorescent sensors that detected the drugs in drug-spiked human serum and blood from patients with malaria, and modified versions of the sensors detected the amount of drug in a dissolved, crushed piperaquine tablet. This assay could help improve tracking of antimalarial drug use and parasite resistance.

ARTICLE TOOLS http://stm.sciencemag.org/content/13/585/eabe1535

SUPPLEMENTARY MATERIALS http://stm.sciencemag.org/content/suppl/2021/03/15/13.585.eabe1535.DC1

RELATED CONTENT
http://stm.sciencemag.org/content/scitransmed/11/473/eaau3174.full
http://stm.sciencemag.org/content/scitransmed/11/521/eaav1636.full
http://stm.sciencemag.org/content/scitransmed/12/554/eaax2550.full
http://stm.sciencemag.org/content/scitransmed/11/510/eaas9917.full
http://stm.sciencemag.org/content/scitransmed/9/387/eaad9735.full

REFERENCES This article cites 44 articles, 8 of which you can access for free
http://stm.sciencemag.org/content/13/585/eabe1535#BIBL

PERMISSIONS http://www.sciencemag.org/help/reprints-and-permissions

Use of this article is subject to the Terms of Service

Science Translational Medicine (ISSN 1946-6242) is published by the American Association for the Advancement of Science, 1200 New York Avenue NW, Washington, DC 20005. The title *Science Translational Medicine* is a registered trademark of AAAS.

Copyright © 2021 The Authors, some rights reserved; exclusive licensee American Association for the Advancement of Science. No claim to original U.S. Government Works

Downloaded from http://stm.sciencemag.org/ by 60259981 on March 17, 2021